Spectra and correlations of climate data from days to decades

Rudolf O. Weber, Peter Talkner

Angaben zur Veröffentlichung / Publication details:

Weber, Rudolf O., and Peter Talkner. 2001. "Spectra and correlations of climate data from days to decades." *Journal of Geophysical Research: Atmospheres* 106 (D17): 20131–44. https://doi.org/10.1029/2001jd000548.

JOURNAL OF GEOPHYSICAL RESEARCH, VOL. 106, NO. D17, PAGES 20,131–20,144, SEPTEMBER 16, 2001

Spectra and correlations of climate data from days to decades

Rudolf O. Weber, and Peter Talkner

Paul Scherrer Institute, Villigen, Switzerland

Abstract. The correlations of several daily surface meteorological parameters such as maximum, minimum, and mean temperature, diurnal temperature range, pressure, precipitation, and relative air humidity are analyzed by partly complementary methods being effective on different timescales: power spectral analysis, second- and higher-degree detrended fluctuation analysis, Hurst analysis, and the direct estimation of the autocorrelation in the time domain. Data from American continental and maritime and European low-elevation and mountain stations are used to see possible site dependencies. For all station types and locations, all meteorological parameters show correlations from the shortest to the longest statistically reliable timescales of about three decades. The correlations partly show a clear power law scaling with site-dependent exponents. Mainly, the short-time behavior of the correlations depends on the station type and differs considerably among the various meteorological parameters. In particular, the detrended fluctuation and the Hurst analyses reveal a possible power low behavior for long timescales which is less well resolved or even may remain unrecognized by the classical power spectral analysis and from the autocorrelation. The long-time behavior of the American temperatures is governed by power laws. The corresponding exponents coincide for all temperatures except for the daily temperature range with different values for the maritime and the continental stations. From the European temperatures those from low-elevation stations also scale quite well, whereas temperatures from mountain stations do not.

1. Introduction

On the Earth, weather and climate show a complicated dynamics being effective on a large variety of timescales. Various methods are available to characterize and quantify the variability of these data. This paper examines the power spectra, correlations and other more recently developed tools characterizing the time variability of several climatological parameters from various locations on the Northern Hemisphere in the twentieth century. It is intended to give a descriptive overview of the temporal correlation patterns of these parameters but does not address the important question about possible physical reasons for the observed scaling behavior. Taking the fact that the scaling behavior of the seemingly much simpler phenomenon of homogeneous turbulence has not yet been fully understood, we do not expect a quick answer to this question. We think, however, that the observed correlation patterns provide a valid basis for tests of existing and future climate and weather models. Any reliable climate model should reproduce these distinctive empirical features of climate dynamics.

The paper is organized as follows: In section 2, qualitative descriptions of the methods used are given, and previously obtained results for meteorological data are shortly reviewed. A description of the data is presented in section 3, followed by sections 4 and 5 giving short technical outlines of the relevant methods and their mutual relations. The results of these methods are described in section 6 for temperature data and in section 7 for other meteorological parameters. In the final section 8 the various findings are summarized and compared.

Paper number 2001JD000548.
0148-0227/01/2001JD000548$09.00

2. Correlation Measures for Meteorological Data

A classical tool of time series analysis is the spectral analysis that allows one to estimate the power spectral density $S(f)$. It is the strength with which a harmonic signal contributes to the considered data as a function of its frequency [*Priestley*, 1981]. *Mitchell* [1976] and *Pelletier* [1997] present power spectra of temperatures covering a range from a day to a million years. The most reliable information can be obviously obtained about

the high-frequency part corresponding to a time range from days to decades. In this time range the meteorological data also show a pronounced site variability. For example, *Pelletier* [1997] distinguishes continental and maritime stations. For daily temperatures, taken as the algebraic mean of the daily minimum and maximum temperatures, he finds power laws for the power spectrum in the high-frequency region for both station types. For maritime stations the power spectrum goes as $S(f) \propto f^{-0.63}$ from the highest frequency, $f = 0.5$ d^{-1}, down to $f = 0.0002$ d^{-1}. For continental stations it goes as $S(f) \propto f^{-1.37}$ for the highest frequencies, $f > 0.03$ d^{-1}, and changes to another power law, $S(f) \propto f^{-0.37}$, for lower frequencies. For 20 Hungarian stations, *Jánosi and Vattay* [1992] found no scaling behavior of temperature power spectra within the available frequency range. They rather propose a stretched exponential shape of the power spectrum.

An algebraic behavior of the power spectral density within a frequency range of more than 1 order of magnitude indicates that roughly speaking the considered time series is self-similar within the corresponding range of times, i.e., that the same features being characteristic on one timescale can be recovered on another timescale upon a multiplication of the signal by an appropriate factor. This literally would be the case for a deterministic fractal curve, but here it is to be understood in a statistical sense only. Moreover, one must be aware that different statistical measures may lead to different scaling behaviors. Signals behaving in this way are called multifractal processes [*Feder,* 1988]. They are characterized by a whole spectrum of scaling exponents. A special case are self-similar processes such as Gaussian fractional Brownian motion, $Y(t)$ [*Mandelbrot and Van Ness,* 1968], which are characterized by a single scaling exponent: A scaling of time t by a factor $u > 0$ can be compensated by a rescaling of the magnitude of the process by the factor u^{ζ}:

$$Y(ut) \sim u^{\zeta} Y(t) \tag{1}$$

where "$\sim$" means equality in distribution; that is, all joint multitime distributions of the considered process are invariant under an appropriate joint rescaling of the process amplitude and time. The scaling exponent ζ of a self-similar process coincides with the Hurst exponent H [*Hurst,* 1951] to which we will come back.

The well-known Wiener Khinchin theorem relates the power spectral density and the autocorrelation function by cosine transforms [*Priestley,* 1981]. In this sense, the two functions contain identical information. Their statistical estimates, however, are of a very different nature. In particular, the long-time behavior of a stationary time series is difficult to characterize by the autocorrelation function because it typically decreases with time and might soon fall below the level that reliably can be detected. Other effects superimposed to scaling, like oscillations, may mask a scaling behavior of the autocorrelation function even if it is dominant at long times.

Complementary to power spectral analysis and to the analysis of the autocorrelation function, new tools have been developed to uncover a possible scaling behavior of a time series [*Peng et al.*, 1992, 1994]. In these methods a running sum is applied to the time series resulting in a new nonstationary time series which resembles a random walk with specific growth properties. In this way the information originally hidden in the long-time tails of the autocorrelation function is transferred onto the growth properties of the auxiliary random walk. These growth properties can be characterized by different variability measures. In the so-called fluctuation analysis (FA) [*Peng et al.,* 1992] the average squared spread of the random walk over a time lag as a function of this lag is taken as a variability measure, while in the so-called detrended fluctuation analysis (DFA) [*Peng et al.,* 1994], a local trend is first subtracted and only then the average squared spread is determined. For the technical details of DFA, see section 4. These measures can be expressed in terms of the power spectral density of the original time series and in this sense are equivalent notions being fully explained by the second-order statistics of the considered process [*Talkner and Weber,* 2000]. However, FA and DFA provide self-averaging measures in contrast to spectral analysis which requires an ad hoc averaging of the periodogram. Moreover, FA and DFA are quite insensitive to the finiteness of the time series and DFA is unaffected by a linear trend of the time series. *Koscielny-Bunde et al.* [1996] applied DFA to daily noon temperatures of two U.S. stations and report a scaling corresponding to a $f^{-0.3}$ law in the power spectrum for timescales from 20 to 1000 days. A similar scaling law with an exponent of about 1/3 was confirmed for daily maximum temperatures from several locations on the globe [*Koscielny-Bunde et al.*, 1998a, 1998b]. On the basis of these analyses, *Koscielny-Bunde et al.* [1998b] propose a universal persistence law of atmospheric variability. Similar scaling exponents were also obtained for daily minimum and maximum temperatures as well as for the daily mean temperature at different stations in the Alpine region [*Talkner and Weber,* 2000]. A main advantage of DFA lies in the fact that it allows the detection of long-range correlations up to time lags of at least one third of the length of the time series. Power spectral analysis and, to an even higher extent, the direct estimation of the autocorrelation function in the time domain are limited to much shorter time lags.

The Hurst analysis [*Hurst,* 1951] is also based on the running sum of the time series under investigation. Here the maximum spread of the random walk within a given time is compared to the standard deviation of the original time series for the same time. For self-similar processes, as defined in equation (1), the scaling exponents resulting from the Hurst analysis, from spectral analysis, fluctuation analysis, and

DFA are strictly related to each other. In general, even if scaling is observed by means of both Hurst analysis and DFA, the two methods need not give the same exponents. The Hurst analysis has been applied to a wide variety of data coming from diverse fields as hydrology, physics, physiology, and economics [*Mandelbrot and Wallis*, 1969; *Bassingthwaighte et al.*, 1994; *Feder*, 1988; *Stanley et al.*, 1999]. To our best knowledge, there does not exist a systematic investigation of meteorological parameters by the Hurst analysis. The method used by *Tsonis et al.* [1998] to estimate the Hurst exponent of global temperature records actually does not use the original standardized Hurst range [*Hurst*, 1951; *Mandelbrot and Wallis*, 1969] but the variability measure of fluctuation analysis. The two measures will produce the same scaling exponent only for self-similar processes.

For the present data, we find, in all cases where scaling is observed, mostly small differences between the Hurst and the DFA exponents, though the significance of these differences often is not obvious; see sections 6 and 7 below. To clarify this question, we introduced a novel method that we call pth-degree DFA where p is a real number. For $p = 2$ we recover the usual DFA. Though p might be any real number, we here restrict ourselves to $p = 3, 4$. In this way we could identify some of the meteorological time series as self-similar and others as multifractal processes.

In previous papers, different types of daily mean temperature or single time readings were used. However, it was shown that the way of calculating the daily mean can lead to different long-term trends [*Weber*, 1993]. Furthermore, it has become evident that the power spectra of daily extreme temperatures may significantly differ from the power spectra of daily mean temperatures [*Talkner and Weber*, 2000]. Thus care must be taken which type of temperature reading or temperature mean is analyzed.

Besides temperature itself, also the diurnal temperature range (DTR) has gained interest as it was found that the DTR has changes over timescales of decades [*Karl et al.* 1984, 1991; *Easterling et al.* [1997]. In the present paper, various types of temperature data (see section 6) and other meteorological parameters (see section 7) will be analyzed by means of the above indicated methods, namely, spectral analysis, analysis of the autocorrelation function, second- and higher-degree DFA, and Hurst analysis. All data sets show pronounced correlations up to the maximally observable time range of approximately 30 years. Roughly speaking, one can say that the temperature data from American maritime stations tend to show a more pronounced scaling behavior than American continental and European low-elevation stations, whereas scaling is less pronounced for mountain stations. Often, minimum temperatures and daily temperature ranges show better scaling than maximum temperatures and daily mean temperatures. For the other meteorological parameters, only European stations were available to us. For precipitation and humidity, scaling is very pronounced both for low-elevation and for mountain stations. For pressure, no scaling can unambiguously be identified, maybe little patience is still required and we shall know more after another 50 years.

3. Data

For several Swiss, German, and Austrian stations the daily minimum and maximum temperatures as well as the daily mean temperature, obtained from several fixed-time readings, are available for about a hundred years. Four low-elevation stations, Basel, Bern, Neuchâtel, and Zürich, and three mountain-top stations, Säntis, Sonnblick, and Zugspitze, all three located higher than 2500 m (mean sea level), were selected. These seven stations have nearly contiguous and homogeneous records extending back at least to 1901 [*Weber et al.*, 1994]. A few gaps with missing data were filled by the corresponding values of the mean annual cycle. For some of these stations also daily pressure, precipitation, and relative humidity are available.

A 187-station daily data set with time series from stations in the contiguous United States was compiled by the National Climatic Data Center, with data records extending back 50-100 years. We selected the 20 stations with the largest annual temperature range as pro-

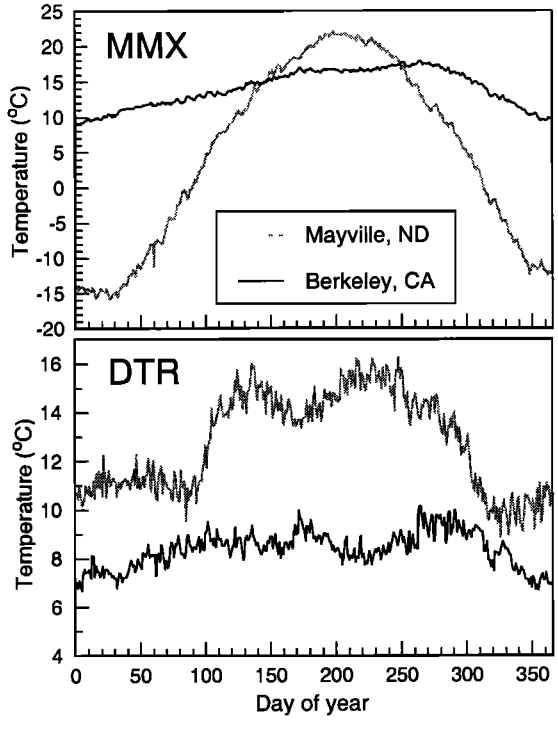

Figure 1. Mean annual cycle of the daily mean temperature (top chart) and the DTR (bottom chart) of the most maritime station, Berkeley, California, (black lines) and of the most continental station, Mayville, North Dakota, (grey lines). The underlying daily mean temperatures are calculated as the arithmetic mean of daily maximum and minimum temperatures.

totypes for continental stations, most of them located in the northern Midwest, and the 20 stations with the smallest annual temperature range as representatives of maritime stations, located both at the West Coast and in the Southeast.

In Figure 1 we show the mean annual cycles of the most continental station, Mayville, North Dakota, with an annual temperature range of 38.1°C, and of the most maritime station, Berkeley, California, with an annual temperature range of 8.8°C. The daily mean temperatures (top chart) closely follow a cosine shape for the continental station and are skewed with a maximum in autumn for the maritime station. For the continental Mayville the first harmonic explains 99 % of variability of the annual cycle but only 89 % for the maritime Berkeley. A detailed discussion of the annual cycle of daily extreme and mean temperatures of many U.S. stations is given by *Shea* [1984]. The DTR (bottom chart) of the maritime station shows a weak annual variation, whereas it varies from about 10°C to 15°C for the continental station. The DTR of the continental station Mayville, North Dakota, has an abrupt transition in April from a low winter value to a higher summer value. This may be caused by less cloud cover during summer, because clouds reduce the DTR by increasing the minimum and reducing the maximum temperature. In June the DTR for Mayville shows a local minimum which presumably is caused by a monsoon effect. These features are still present in the average of 20 continental stations (Figure 2). In particular, the steep increase of the DTR in April and the depression in June remain clearly visible even in this average. For the maritime stations the difference between summer and winter values of DTR is smaller than for the continental stations and the transition between these values is gradual.

For all 40 U.S. stations, segments with many missing values at the beginning and at the end of the record were deleted. The remaining missing values (at most 5% of

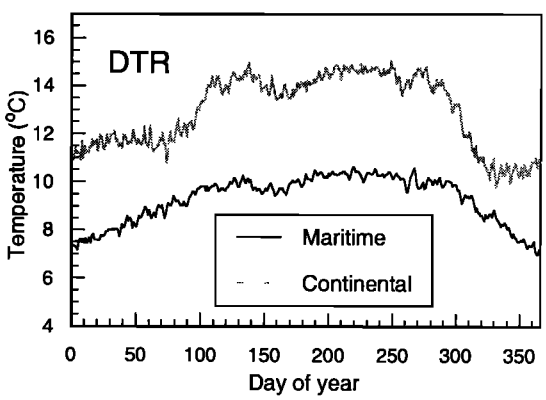

Figure 2. Composite mean of the annual cycle of the DTR for 20 maritime stations (black line) and 20 continental stations (grey lines).

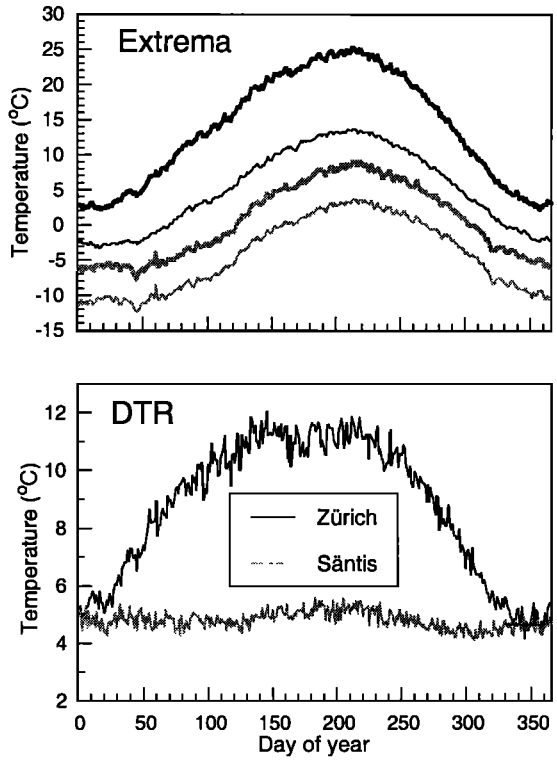

Figure 3. Mean annual cycle of the daily extreme temperatures (top chart) and of the DTR (bottom chart). The thin lines give the minimum temperature, the thick lines indicate the maximum temperature. The grey curves are for the mountain-top station Säntis, the black curves for the low-elevation station Zürich.

the data) were replaced by the corresponding values of the mean annual cycle, which resulted in contiguous data records from 49 to 96 years length.

For all data the annual cycle was removed by calculating the average over all years for each day and subtracting the resulting mean annual cycle from the original data. The resulting fluctuations are used in the further calculations.

In Central Europe the mountain stations, like Säntis, show an almost parallel annual cycle of daily minimum and maximum temperature (top chart of Figure 3). For the low-elevation stations, like Zürich, the maximum temperature rises more strongly in summer than the minimum temperature (top chart of Figure 3), resulting in a pronounced seasonal variation of the DTR (bottom chart of Figure 3). In contrast, the DTR of the mountain stations is almost constant during the year. For the low-elevation stations the smaller DTR values in winter may be partly caused by low-lying clouds ("Hochnebel") whose upper boundaries stay below the height of the mountain stations. Such situations occur frequently during winter in connection with cold air pools in the northern Alpine foreland. This is supported by the investigation of *Dai et al.* [1999] who

showed a strong influence of the cloud cover on DTR because clouds reduce the daily maximum temperature. Moreover, at mountain stations the influence of the free troposphere is felt stronger.

4. Power spectral analysis and detrended fluctuation analysis

The meteorological data under consideration are time series sampled with equidistant time steps of 1 day. Their power spectral density $S(f)$ is calculated by a standard nonparametric technique [*Press et al.*, 1992]. For this purpose the time series is divided into K equally long segments overlapping by one half of their length M. For each segment the periodogram is obtained by applying a Welch filter and using a fast Fourier transform. The periodograms of all segments are averaged, in this way reducing the sampling error of the spectral estimate by a factor of about $9K/11$.

For a stationary time series $x(t)$, the power spectral density $S(f)$ is the Fourier transform of the autocorrelation function $C(\tau) = \langle [x(t+\tau) - \langle x \rangle][x(t) - \langle x \rangle] \rangle$ of the signal,

$$C(\tau) = \int_0^\infty df S(f) \cos(2\pi f \tau) , \tag{2}$$

where τ is a time lag and the angular brackets denote an ensemble average. The power spectral density in (2) is normalized such that the total power is contained in the positive frequencies. If the autocorrelation decays algebraically for times larger than τ_0 with an exponent α, one also finds a scaling behavior of the power spectrum with another exponent β in the corresponding frequency range $f < 1/\tau_0$, and vice versa; that is,

$$C(\tau) \propto \tau^{-\alpha} \Longleftrightarrow S(f) \propto f^{-\beta} \text{ for } 0 < \alpha, \beta < 1 . \tag{3}$$

The two exponents are related by $\beta = 1 - \alpha$. For autocorrelation functions decaying faster than τ^{-1} the power spectrum approaches a constant value in the limit $f \to 0$; that is, $\beta = 0$.

There is no direct relation between the power spectrum at high frequencies and the behavior of the autocorrelation function at short timescales.

In DFA [*Peng et al.*, 1994] a running sum of the observed variable x_i, $i = 1, \ldots, N$ is calculated, $y(n) = \sum_{i=1}^{n} x_i$, where $n = 1, \ldots, N$. The time series of the $y(n)$ is divided into nonoverlapping segments of length s. Within each segment k the linear regression $\tilde{y}_{k,s}(n) = m_k n + b_k$ of the random walk $y(n)$ is performed and is subtracted from the random walk on that segment. The detrended squared variability $F^2(s)$ of the signal is defined by

$$F^2(s) = \frac{1}{s+1} \overline{\sum_{n=(k-1)(s+1)+1}^{k(s+1)} [y(n) - \tilde{y}_{k,s}(n)]^2} , \tag{4}$$

where the bar denotes the average over all segments. This quantity measures the variability of the original signal at timescales smaller than the segment length s. A more detailed discussion of the variability $F^2(s)$ and of its relationship to the power spectral density $S(f)$ and the autocorrelation function $C(\tau)$ was given recently [*Talkner and Weber*, 2000].

For white noise with $C(t - t') = \sigma^2 \delta(t - t')$, the squared variability increases linearly in s:

$$F^2(s) = \sigma^2 s . \tag{5}$$

For a time series with an algebraically decaying autocorrelation function, $C(\tau) \propto \tau^{-\alpha}$, for $\tau > \tau_0$, the variability increases with a power law,

$$F_2(s) \equiv (F^2(s))^{1/2} \propto s^{\gamma_2} , \tag{6}$$

where the exponents γ_2 and α are related by

$$\gamma_2 = \begin{cases} 1 - \alpha/2 & \text{for } 0 < \alpha < 1 \\ 1/2 & \text{for } \alpha > 1. \end{cases} \tag{7}$$

The analysis of synthetic data with given spectral properties shows that the variability $F_2(s)$ can be reliably estimated up to a time lag of at least one third of the length of the time series [*Talkner and Weber*, 2000].

We suggest here a whole family of variability measures constructed in an analogous way as higher-order structure functions in the analysis of turbulent data [*Monin and Yaglom*, 1965]. Instead of taking the second power of the random walk deviation from its local trend, one may consider an arbitrary power p of the absolute value of this deviation:

$$F^p(s) = \frac{1}{s+1} \overline{\sum_{n=(k-1)(s+1)+1}^{k(s+1)} |y(n) - \tilde{y}_{k,s}(n)|^p} . \tag{8}$$

We shall call its pth root the pth-degree DFA variability: $F_p(s) = (F^p(s))^{1/p}$. It must not be confused with higher-order DFA which is of second degree in our notation but uses a higher-order nonlinear trend [*Bunde et al.*, 2000] or with higher-order wavelet methods [*Koscielny-Bunde et al.*, 1998b]. Here we shall only consider the cases $p = 3, 4$ in addition to the standard second power.

If the correlation function of the original process decays algebraically for large times and if the auxiliary random walk is self-similar for large times, i.e., if it scales according to equation (1) with an exponent ζ, then the pth-degree DFA scales with an exponent that is independent of the degree p:

$$F_p(s) \propto s^{\gamma_2}, \tag{9}$$

where $\gamma_2 = \zeta = 1 - \alpha/2$ for $0 < \alpha < 1$. In the more general case of a multifractal process $F_p(s)$ is still expected to scale in s, $F_p(s) \propto s^{\gamma_p}$, but with an exponent γ_p that depends on p.

5. Hurst Analysis

The Hurst analysis [*Hurst*, 1951; *Mandelbrot and Wallis*, 1969] is also based on the division of the running sum $y(n)$ into nonoverlapping segments $(n_0, n_0 + s)$ of length s. In each segment the straight line connecting the first and the last point is determined, $y_l = (y(n_0 + s) - y(n_o))/s(n - n_0) + y(n_0)$, subtracted from the running sum, and the difference $R(n_0, s)$ between the absolute maximum and absolute minimum on the considered segment is calculated:

$$R(n_0, s) = \max_{n0 \le n \le n_0 + s} [y(n) - y_l(n)] - \min_{n0 \le n \le n_0 + s} [y(n) - y_l(n)] \; . \quad (10)$$

This range is normalized by the standard deviation $\sigma(n_0, s)$ of the original process on the considered segment,

$$\sigma^2(n_0, s) = \sum_{n=n_0}^{n_0+s} \left[x(n) - \sum_{n=0}^{n_0+s} x(n)/s \right]^2 /(s-1) \quad (11)$$

and, finally, averaged over over all segments of length s:

$$R(s) = \overline{R(n_0, s)/\sigma(n_0, s)} \; . \quad (12)$$

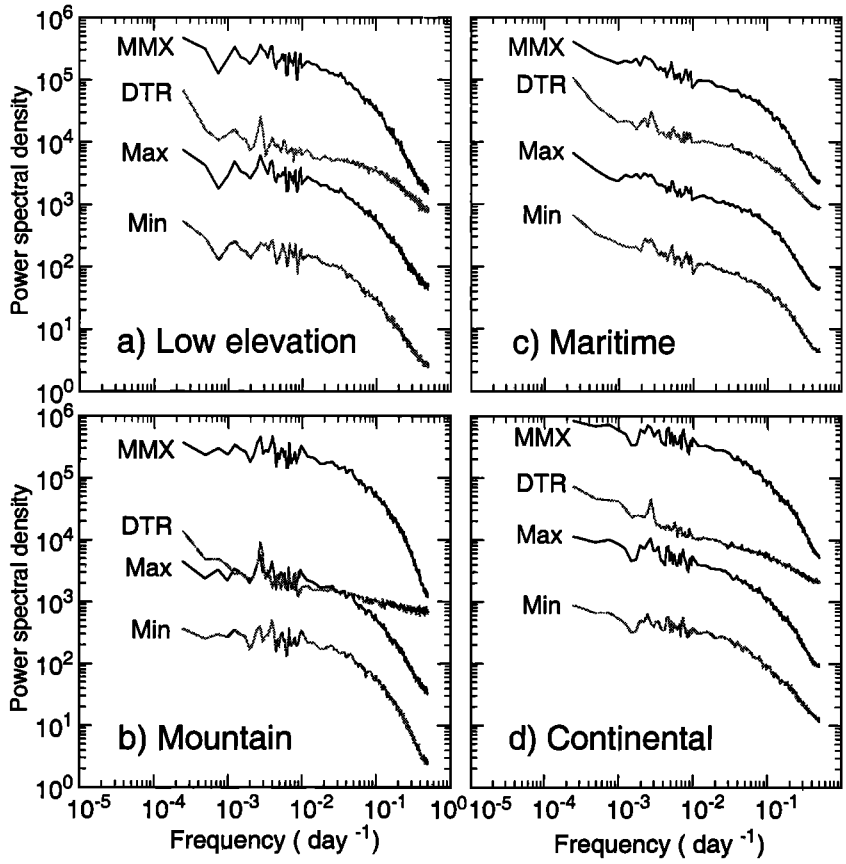

Figure 4. Composite power spectra of the (a) four low-elevation stations Basel, Bern, Neuchâtel, and Zürich, (b) the three mountain-top stations Säntis, Sonnblick and Zugspitze, (c) the 20 U.S. maritime stations, and (d) 20 U.S. continental stations as described in text. From bottom to top, the power spectra of the daily minimum, the maximum temperature, the DTR, and the arithmetic mean of maximum and minimum temperatures (MMX) are shown. To better separate the curves, the spectra are shifted by one decade from each other, with the spectral density of the minimum temperature being truly scaled in units of $(°C)^2$ d^{-1}. The high-frequency part, $f > 0.01$ d^{-1}, is calculated from segments of lengths of 512 days, and the low-frequency part, $f < 0.01$ d^{-1}, from segments of lengths of 4096 days, hence the scatter of the low-frequency part is larger than that of the high-frequency end of the spectrum. The logarithmic scales on both axes allows one to identify scaling regions as the linear parts of the graph; the slopes give the respective scaling exponents.

Table 1. Algebraic Scaling Exponents β of Power Spectral Density

Station Type	MMX		DTR		Maximum		Minimum	
	$f < 0.1$	$f > 0.1$	$f < 0.1$	$f > 0.1$	$f < 0.1$	$f > 0.1$	$f < 0.1$	$f > 0.1$
Low elevation	0.25 (0.20)	2	0.35 (0.32)	1	0.25 ([0.16])	1.5	0.25 ([0.20])	1.5
Mountain	[0.10] ([0.06])	3	[0.25] (—)	0.25	[0.20] ([0.10])	2	[0.20] (0.08)	2
Continental	[0.25] (0.24)	2	0.40 (0.44)	0.5	0.30 (0.26)	2	0.25 (0.26)	1.25
Maritime	0.30 (0.32)	2	0.35 (0.36)	1.25	0.35 ([0.32])	2	0.35 ([0.34])	2

MMX stands for the arithmetic mean of daily minimum and maximum temperature. DTR denotes the difference of daily maximum and minimum temperature. Frequency ranges are given in units of 1/day. The numbers in parentheses are calculated from the scaling exponent of the DFA method. Numbers in brackets indicate that scaling is not well pronounced, and hence the exponent given is only a rough estimate.

If this standardized range scales, the corresponding exponent H is known as the Hurst exponent and $R(s)$ becomes

$$R(s) \propto s^H . \tag{13}$$

For a self-similar random walk $y(n)$, the Hurst exponent agrees with both the exponent ζ of the random walk and the DFA exponent γ_2: $H = \zeta = \gamma_2$. These relations, however, are restricted to fractional Brownian motion and other self-similar processes which observe the scaling relation (1) in distribution. For multifractal processes, H and γ_p will differ from each other.

Finally, we note that the different variability measures, such as the power spectrum, DFA variabilities, Hurst range, etc., were separately determined for each single station and only then averages were performed over stations of the same type. For DFA and Hurst analysis, double logarithmic plots were performed from these average variability measures. We have also interchanged the order of the last two steps, i.e., averaged the logarithmic variabilities, however, without any significant change of the results.

6. Fluctuations of Characteristic Temperatures

The power spectra of daily minimum, maximum, and mean temperatures (see Figure 4) qualitatively show the same behavior for all groups of stations. There is a slow decrease at low frequencies and a steeper decrease toward the Nyquist frequency $f = 0.5$ d^{-1}. In all cases the transition between the two regimes occurs at a frequency corresponding to approximately 1 month. The low- and high-frequency behavior can be described by scaling exponents which for the different station types are listed in Table 1. *Pelletier* [1997] found for maritime stations a single scaling law for all frequencies with an exponent $\beta = 0.63$. The difference between his and our findings ($\beta = 0.3 - 0.4$) is presumably caused by the

Table 2. Scaling Exponents of DFA and Hurst Exponent for Low-Elevation Stations

	MMX	DTR	Maximum	Minimum	Pressure	Precipiation	Humidity
γ_2	0.60	0.66	[0.58]	[0.60]	[0.56]	0.54	0.68
γ_3	0.59	0.66	[0.58]	[0.59]	[0.55]	0.54	0.68
γ_4	0.59	0.66	[0.58]	[0.57]	[0.53]	0.53	0.68
H	0.62	0.70	[0.61]	[0.63]	[0.59]	0.57	0.69
$\Delta\gamma_{32}$	0.005	[0]	0	-0.01	-0.013	—	0
$\Delta\gamma_{42}$	0.01	[0]	0	-0.02	-0.024	—	0
$\Delta H2$	[0.04]	[0]	0.037	—	0.036	0.03	0.008
	mfp	ssp	ssp				ssp

MMX stands for the arithmetic mean of daily minimum and maximum temperature. DTR denotes the difference of daily maximum and minimum temperature. γ_p, $p = 2, 3, 4$ denote the pth-degree DFA exponent and H the Hurst exponent. $\Delta\gamma_{p2}$, $p = 3, 4$ indicate the algebraic growth exponent of the ratio between the pth-degree DFA and the second-degree DFA. $\Delta H2$ is accordingly defined as the exponent of the ratio between the Hurst analysis and second-degree DFA. Numbers in brackets indicate that scaling is not well pronounced, and hence the exponent given is only a rough estimate. The last line contains comments about the particular nature of scaling: mfp stands for multifractal process, and ssp for self-similar process; there is no comment for parameters showing only weak scaling or no scaling.

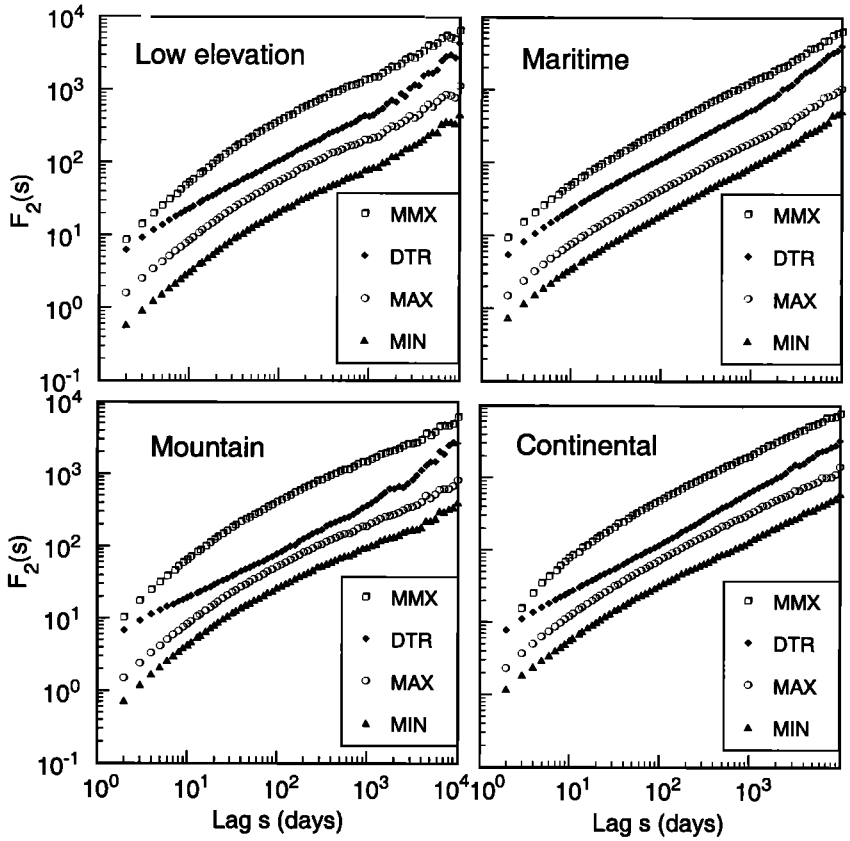

Figure 5. Variability (4) of the DFA as a function of segment length. The composite means of the same four groups of stations as in Figure 4 are shown. For better readability of the plots the curves are shifted by arbitrary factors.

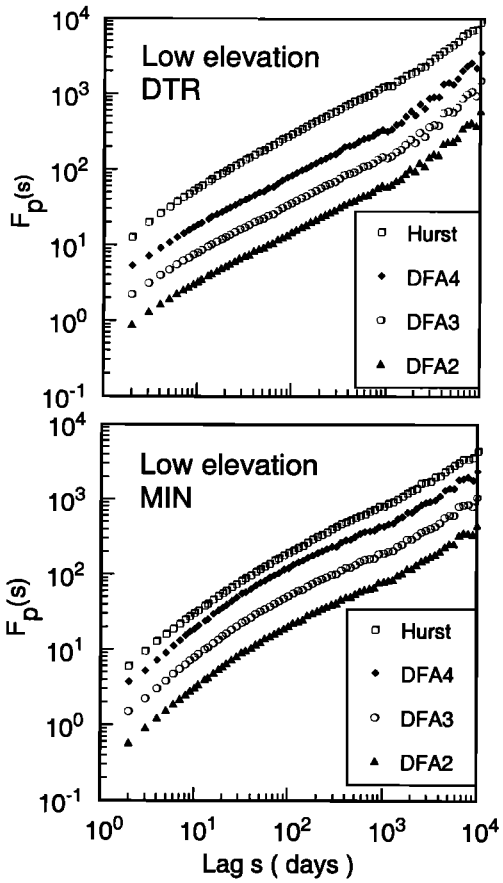

different ways of eliminating the annual cycle. *Pelletier* [1997] only subtracted the first harmonic of the annual cycle, whereas we removed the full annual cycle, including all higher harmonics.

For all station types the power spectrum of DTR falls off with a much lower rate at high frequencies than the power spectra of the extreme and the mean temperatures; that is, the DTR has a much higher variability at short times. For low-elevation and maritime stations the decay is faster at high frequencies than at low frequencies, whereas for mountain and continental stations, the same scaling law applies for the whole frequency range. The scaling exponents are given in Table 1. The uncertainties, in particular that of the low-frequency exponents, apparently are quite large.

The scaling behavior at low frequencies, i.e., for large timescales, can also be observed by the DFA, whose results are plotted in Figure 5. In all cases the variability $F_2(s) = \left(F^2(s)\right)^{1/2}$ increases stronger than with the square root of s, because it would result for an uncorrelated random signal (white noise). Thus the temper-

Figure 6. The pth-degree DFA variabilities $F_p(s)$ (8) for $p = 2, 3, 4$, and the Hurst range $R(s)$ (12) as a functions of the segment length for low-elevation DTR and low-elevation minimum temperatures.

Table 3. Scaling Exponents of DFA and Hurst Exponent for Mountain Stations

	MMX	DTR	Maximum	Minimum	Pressure	Precipitation	Humidity
γ_2	[0.53]	—	[0.55]	[0.54]	[0.60]	0.64	0.64
γ_3	[0.53]	—	[0.55]	[0.54]	[0.59]	0.64	0.64
γ_4	[0.53]	—	[0.55]	[0.54]	[0.58]	0.65	[0.65]
H	[0.55]	0.65	0.57	[0.57]	[0.62]	0.64	0.66
$\Delta\gamma_{32}$	[0]	—	-0.005	-0.005	-0.01	[0.002]	[-0.005]
$\Delta\gamma_{42}$	[-0.01]	—	-0.01	-0.01	-0.016	[0.01]	[-0.01]
$\Delta H2$	0.036	—	0.03	0.04	0.03	-	-

Symbols used are the same as in Table 2, as described there. None of the processes can be unambiguously identified as self-similar or multifractal.

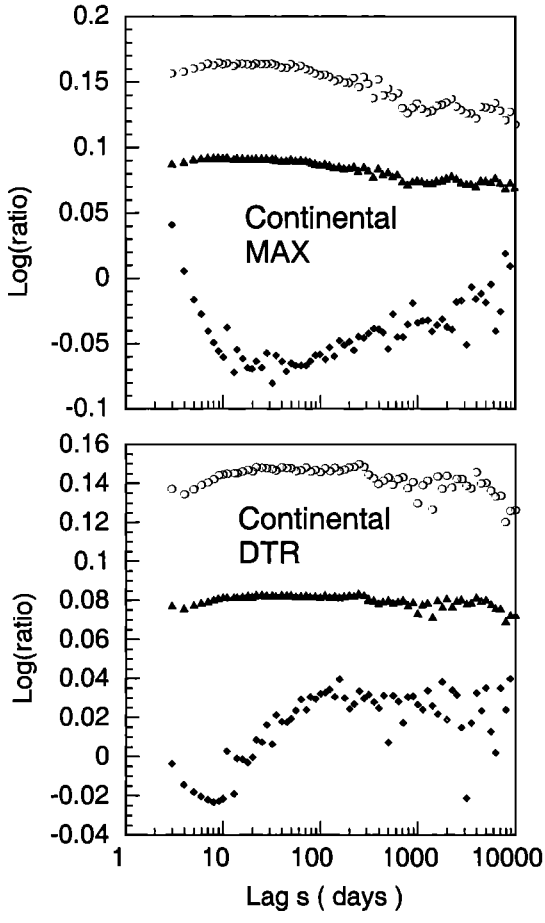

Figure 7. Logarithm (base 10) of the ratio of the third- to second-degree (triangles), of the fourth- to second-degree (circles) variabilities and of the Hurst range to the second-degree variability (diamonds) as a function of the segment length for continental maximum temperatures, and for continental DTR. Note that for the maximum temperatures the third- to second-degree ratios and the fourth- to second-degree ratios decrease according to a power law over 2 to 3 orders of magnitude of the lag s for the maximum temperatures, whereas the Hurst to second-degree ratios increase with a power low. In contrast, the same ratios for the DTR stay almost constant for 2 to 3 orders of magnitudes of time lags. The Hurst ratios are shifted by factors of 1.25 and 1.1 for maximum temperatures and DTR, respectively.

ature data for all stations show correlations up to the longest observable timescales.

For the maritime stations the variabilities $F_2(s)$ of all temperature types follow almost perfect power laws over two to three decades up to the longest time lags. Only for the DTR a significantly steeper increase sets in for long time lags; that is, at large times the correlations of the DTR decay at a slower rate than at smaller times. A qualitatively similar behavior is observed for the low-elevation and continental stations, although, there, stronger deviations from scaling are apparent. For the mountain stations only the maximum scales, whereas the variabilities of all temperature types appear as almost everywhere curved in a doubly logarithmic plot. They are not described by scaling laws.

A similar picture as for the second-degree results in the third and fourth-degree DFA and Hurst analysis; see Figure 6. In most cases the three different degrees of DFA run almost parallel and, as far as scaling is present, apparently yield exponents that come rather close to those of self-similar processes, i.e. $\gamma_p \approx \gamma_2$ for $p = 3, 4$. To reveal also a small dependence of γ_p on p, we made a ratio test; that is, we plotted the ratios of the logarithms, $\log F_p(s)/\log F_2(s)$, as functions of the logarithm of s. For a strictly self-similar process a constant would result. In Figure 7 a few representative examples are given. In Tables 2, 3, 4 and 5 we give the scaling exponents γ_p and indicate the cases that are self-similar and those for which a significant difference between the exponents γ_p for $p = 2, 3, 4$ was found by the ratio test. The maritime stations, again, show very good scaling except for the maximum temperatures in the third- and fourth-degree variability. For the low-elevation stations the Hurst analysis shows scaling for all temperature types, whereas third- and fourth-degree DFA shows scaling only for the DTR with clear deviations at short and long time lags. Similarly, the Hurst analysis reveals scaling for all temperature types except for the maximum temperatures of the continental stations, whereas third- and fourth-degree DFA reveals scaling only for minimum temperatures and DTR. In the latter case the scaling behavior is very pronounced over four decades. For the mountain stations, only the Hurst analysis shows scaling for DTR.

Table 4. Scaling Exponents of DFA and Hurst Exponent for Continental Stations

	MMX	DTR	Maximum	Minimum
γ_2	0.62	0.72	0.63	0.63
γ_3	0.61	0.71	[0.63]	0.61
γ_4	0.59	0.71	0.62	0.60
H	0.65	0.71	0.66	0.65
$\Delta\gamma_{32}$	-0.012	0 -0.010	[0]	-0.015
$\Delta\gamma_{42}$	-0.024	0	-0.016	-0.03
$\Delta H2$	0.03	0	0.025	0.03
	mfp	ssp		mfp

Symbols as in Table 2.

At high frequencies the power spectra of the different temperature elements scale with quite different exponents (Table 1) for the four station types. As the high-frequency behavior of the power spectrum does not fully determine the autocorrelation at short time lags, we also consider the autocorrelation in the time domain up to 50 days. Figure 8 shows the autocorrelation functions for the extreme temperatures and the DTR for the four groups of stations. The autocorrelations of the maximum temperature decay in a very similar way for the Central European and the North American stations.

Within the first six days, maritime and continental minimum temperatures decorrelate according to the same power law with an exponent of approximately $\alpha = 0.7$. For longer time lags this correlation decay persists for the maritime stations, while the decorrelation is much stronger for the continental stations. The higher persistence at maritime stations presumably is caused by the ocean acting as a thermostat. A similar but more gradual difference is seen for mountain and low-elevation stations. There, low-lying clouds and/or latent heat exchange of the surface are probable causes for this difference. Already, at a lag of 1 day, the DTR is much weaker correlated than the daily extreme temperatures. For all time lags the DTR has a higher autocorrelation for low-elevation stations than for mountain stations and for maritime stations than for continental stations.

7. Pressure, Precipitation, and Air Humidity

For most European stations, daily pressure, precipitation, and relative air humidity (short: humidity) data are available for the twentieth century. The annual cycles of these data were determined in the same way as for the temperature data and were removed from the data.

The power spectra of pressure (Figure 9) are qualitatively similar to the spectra of minimum and maximum temperatures and can be characterized by two scaling regions for low and high frequencies. The corresponding scaling exponents are listed in Table 6. The same two scaling regions may also be observed for precipitation and humidity (Figure 9), however, the decay at high frequencies is much weaker than that for pressure. The total variance of precipitation and humidity at mountain stations is considerably higher than at low-elevation stations. Presumably, the humidity at low elevations is preserved from large fluctuations by the compensating influence of the vegetation.

Table 5. Scaling Exponents of DFA and Hurst Exponent for Maritime Stations

	MMX	DTR	Maximum	Minimum
γ_2	0.66	0.68	[0.66]	[0.67]
γ_3	0.65	0.68	[0.66]	[0.66]
γ_4	0.66	0.68	[0.66]	[0.65]
H	0.69	0.69	[0.68]	[0.70]
$\Delta\gamma_{32}$	[-0.01]	[0]	[-0.005]	-0.01
$\Delta\gamma_{42}$	[-0.02]	[0]	[-0.01]	-0.02
$\Delta H2$	0.025	[0]	0.017	0.024
		ssp		

Symbols as in Table 2.

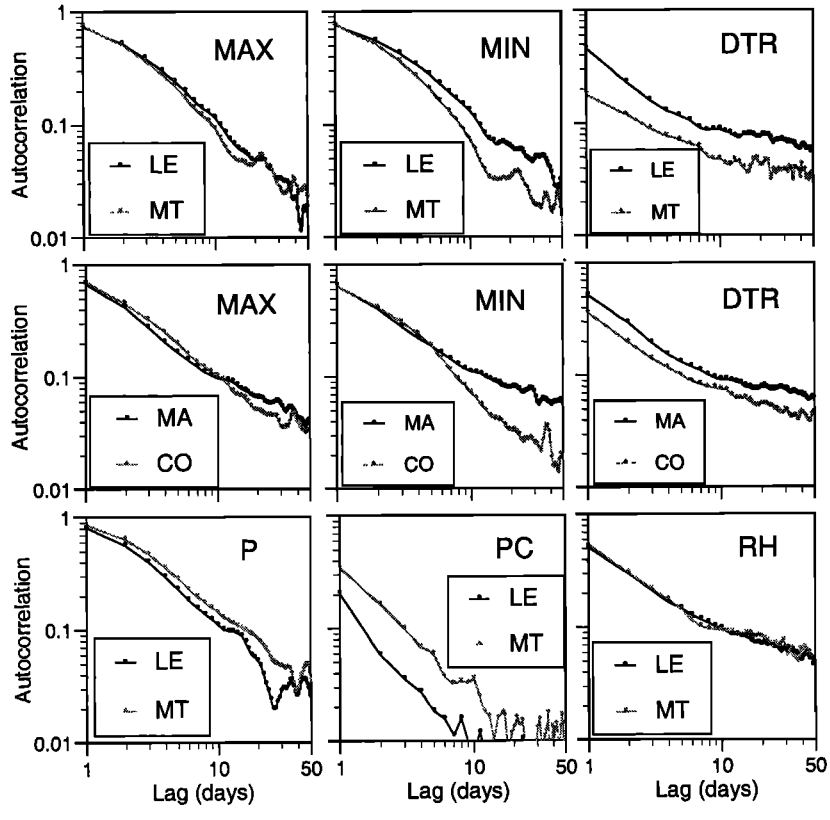

Figure 8. Autocorrelation functions of the the maximum temperature (MAX), the minimum temperature (MIN), and the DTR. The composite means of the same four groups of stations as in Figure 4 are shown. The top charts are for low-elevation (LE) and mountain (MT) stations, and the middle charts for maritime (MA) and continental (CO) stations. For the low-elevation and mountains stations the autocorrelation of pressure (P), precipitation (PC), and humidity (RH) are shown in the bottom charts.

The autocorrelation functions of pressure, precipitation and humidity are shown in Figure 8. For pressure and precipitation the correlations at the mountain stations are higher than those at the low-elevation stations, but otherwise behave almost in parallel. The humidity correlations are practically identical for both station types. Their decay is very slow, comparable to that of the DTR at low-elevation stations.

The results of the second-degree DFA are presented in Figure 10. Precipitation and humidity show a clear power law scaling over two to three decades for both station types. For the mountain stations, humidity shows strong deviations from scaling for large time lags. For low-elevation stations, the scaling regime for pressure starts at larger time lags, no scaling of pressure is found for the mountain stations. The resulting scaling exponents β are listed in Table 6. They agree well with the scaling exponents estimated from the power spectra. *Vattay and Harnos* [1994] analyzed humidity and precipitation data of 25 years from Hungarian stations. They found similar scaling laws as we do here. The exponents of the pth-degree DFA and Hurst analysis, γ_p and H, respectively, are collected in Tables 2 and 3. For low-elevation stations, humidity is likely to be a self-similar process.

8. Conclusions

We investigated various aspects of the variability of the twentieth century's weather and climate on the Northern Hemisphere by different, partly complementary, methods. The analyzed data are daily minimum and maximum temperatures from continental and coastal stations in the United States and from low-elevation and mountain stations in Central Europe as well as daily pressure, relative air humidity, and precipitation data from the European stations. Unfortunately, the latter meteorological parameters have not been available for the American stations. The DTR as the difference of maximum and minimum temperatures provides further information that is not immediately visible from the original temperature data. The employed methods are the spectral analysis, which gives frequency-specific information, DFA of various degrees,

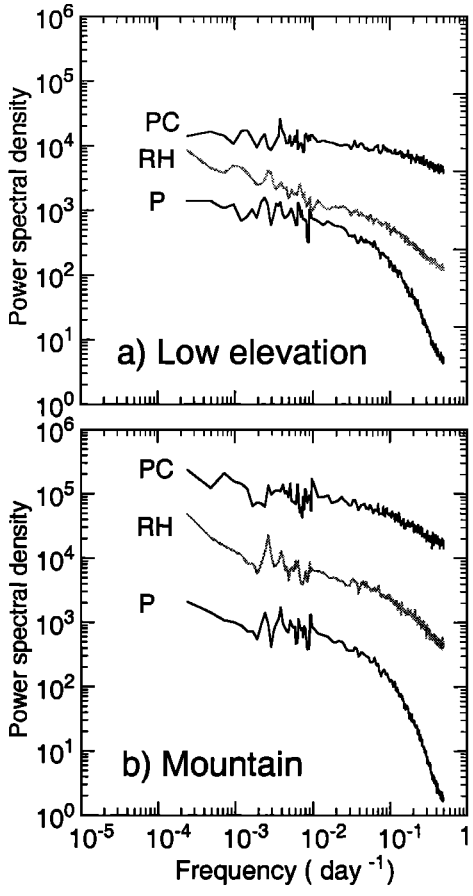

Figure 9. Composite power spectra of the four low-elevation stations Basel, Bern, Neuchâtel, and Zürich (top chart) and the three mountain-top stations Säntis, Sonnblick, and Zugspitze (bottom chart). From bottom to top, the power spectra of the pressure (P), the relative air humidity (RH), and the precipitation (PC) are shown. To better separate the curves, the spectra of humidity are multiplied by 2, the spectra of precipitation by a factor of 100.

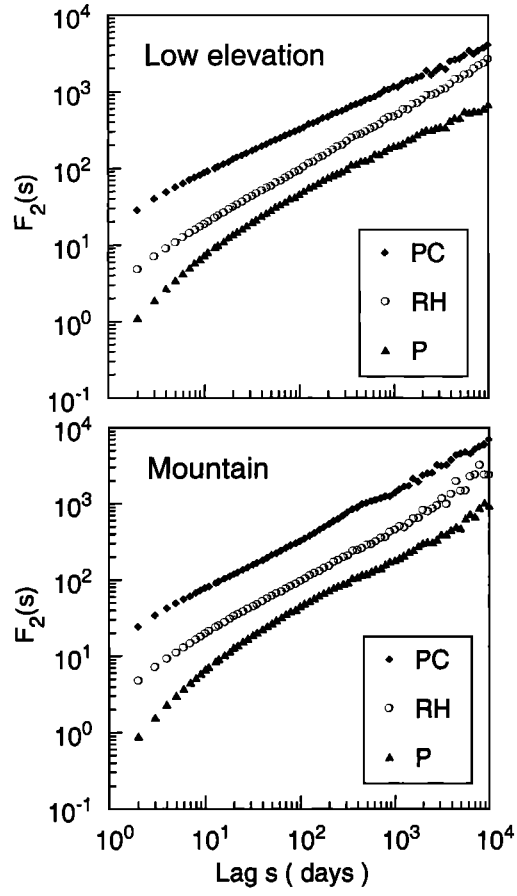

Figure 10. Variability (4) of the DFA as a function of segment length. The composite means of the same two groups of stations as in Figure 9 are shown. For better readability of the plots the curves are shifted by arbitrary factors.

and the Hurst analysis, which indicate long-time correlations and, finally, a direct estimation of the autocorrelations that best describe the short-time behavior. The DFA is tailored to detect a possible scaling behavior at long times and gives reliable results, which are very little influenced by the statistics due to the finite length of the considered time series, at least up to a third of its total length. In the present investigation, in this way, we found correlations for all mentioned meteorological parameters that extend to at least 27 years. For some of the parameters a scaling behavior extends to almost three decades, whereas for other parameters, a power law would provide only a poor model.

As a further method to corroborate a possible scaling of a time series, we applied the Hurst analysis to the

Table 6. Algebraic Scaling Exponents β of Power Spectral Density

	Pressure		Precipitation		Humidity	
Station Type	$f < 0.1$	$f > 0.1$	$f < 0.1$	$f > 0.1$	$f < 0.1$	$f > 0.1$
Low elevation	0.18 (0.12)	3	0.10 (0.08)	0.5	0.42 (0.36)	1
Mountain	[0.2] ([0.2])	3	0.20 (0.28)	0.75	0.36 (0.28)	1

Frequency ranges are given in units of 1/day. Numbers in parentheses are calculated from the scaling exponent of the DFA method, numbers in brackets indicate that scaling is not well pronounced, and hence the exponent given is only a rough estimate.

data. We always find scaling with the Hurst analysis when the DFA also shows scaling. Typically, the resulting Hurst exponent H is slightly larger than the DFA exponent γ_2. To see whether this can be interpreted as an indication of multifractal processes, we performed pth-degree DFA and, in particular, looked for scaling of the ratios of the third- to the second- and fourth- to the second-degree DFA. In this way we found that if the DTR scales, it behaves like a self-similar process, whereas, for example, all other continental temperatures also scale but appear to be multifractal. On the other hand, except for maritime $T_{\min}$ for which the exponents γ_p and H are difficult to estimate, the other maritime temperatures behave almost self-similarly.

Both the mountain temperatures and the other mountain meteorological parameters, except mountain precipitation, which is quite self-similar, do not show clear scaling.

For the low-elevation stations the temperatures only scale for time lags varying over 1.5 orders of magnitude and, in particular, show deviations from the scaling behavior at large time lags. For these stations, also pressure does not scale well. Precipitation and humidity both show pronounced scaling over a wide range and humidity appears to be self-similar.

The scaling exponents γ_2 of all scaling meteorological parameters and for all station types range between 0.54, for low-elevation precipitation, and 0.71, for continental DTR. We think that this quite large scatter of scaling exponents, together with the facts that the type of scaling partly also is of qualitatively different nature and that some parameters do not properly scale at all, sheds some doubt on the claimed universal persistence law governing atmospheric variability [*Koscielny-Bunde et al.*, 1998b]. The extremely high-dimensional and strongly driven dynamical system of the Earth's climate apparently presents to the observer different aspects that show up in the different meteorological parameters and, in particular, also reflect themselves in different station sites. For example, there is a pronounced difference in the behavior of mountain and maritime stations. In the first case, one might assume that the influence of the free atmospheric dynamics is dominant, whereas the presence of an ocean seems to increase the correlations considerably at maritime stations. That these differences yet persist up to the longest observed timescales is indeed very surprising.

As one would expect, the high-frequency behavior is much more dependent on the particular type of parameters and location. Looking at the power spectra, one finds power laws with exponents ranging from $\beta = 0.25$ to 3. More detailed insight may here be gained from the autocorrelation functions. For example, these reflect nicely the high persistency of minimum temperatures up to a month caused by the ocean at maritime stations and, in contrast, the high variability of the free atmosphere that strongly influences the temperature data at the mountain stations.

We would, again, like to emphasize that the various aspects of the climate dynamics that have been revealed by the described methods provide a broad testing ground for existing and future numerical climate models. Only when a model can reproduce these various empirical aspects on both short and long timescales can it be considered as reliable. Once this stage is reached, a deeper physical understanding can be gained by specific variations of the model parameters.

Acknowledgments. Valuable discussions with Remo Badii are gratefully acknowledged. Data were kindly provided by the Deutscher Wetterdienst in Offenbach, the Schwei erische Meteorologische Anstalt in Zurich, the Zentralanstalt für Meteorologie und Geophysik in Vienna, and the National Climatic Data Center in Asheville, N.C.

References

Bassingthwaighte, J. B., L. S. Liebovitch, and B. J. West, *Fractal Physiology*, 364 pp., Oxford Univ. Press, New York, 1994.

Bunde, A., S. Havlin, J. W. Kantelhardt, T. Penzel, J.-H. Peter, and K. Voigt, Correlated and uncorrelated regions in heart-rate fluctuations during sleep, *Phys. Rev. Lett., 85*, 3736-3739, 2000.

Easterling, D. R.,et al., Maximum and minimum temperature trends for the globe, *Science, 277*. 364-367, 1997.

Feder, J., *Fractals*, 283 pp., Plenum, New York, 1988.

Hurst, H. E., Long-term storage capacity of reservoirs, *Trans. Am. Soc. Civ. Eng., 116*, 770-808, 1951.

Jánosi, I. M., and G. Vattay, Soft turbulent state of the atmospheric boundary layer, *Phys. Rev. A, 46*. 6386-6389, 1992.

Karl, T. R., G. Kukla, and J. Gavin, Decreasing diurnal temperature range in the United States and Canada from 1941 through 1980, *J. Clim. Appl. Meteorol., 23*, 1489-1504, 1984.

Karl, T. R., G. Kukla, V. Razuvayev, M. J. Changery, R. G. Quayle, R. R. Heim Jr., D. R. Easterling, and C. B. Fu, Global warming: Evidence for asymmetric diurnal temperature change, *Geophys. Res. Lett., 18*, 2253-2256, 1991.

Koscielny-Bunde, E., A. Bunde, S. Havlin, and Y. Goldreich, Analysis of daily temperature fluctuations, *Physica A, 231*, 393-396, 1996.

Koscielny-Bunde, E., H. E. Roman, A. Bunde, S. Havlin, and H.-J. Schellnhuber, Long-range power-law correlations in local daily temperature fluctuations, *Philos. Mag. B, 77*, 1331-1340, 1998a.

Koscielny-Bunde, E., A. Bunde, S. Havlin, H. E. Roman, Y. Goldreich, and H.-J. Schellnhuber, Indication of a universal persistence law governing atmospheric variability, *Phys. Rev. Lett., 81*, 729-732, 1998b.

Mandelbrot, B. B., and J. W. Van Ness, Fractional Brownian motions, fractional noises and applications, *SIAM Rev., 5*, 422-437, 1968.

Mandelbrot, B. B., and J. R. Wallis, Some long-run properties of geophysical records, *Water Resour. Res., 5*, 321-340, 1969.

Mitchell, J. M., Jr., An overview of climatic variability and its causal mechanisms, *Quat. Res., 6*, 481-493, 1976.

Monin, A. S., and A. M. Yaglom, *Statistical Fluid Mechanics: Mechanics of Turbulence*, vol. 2, 874 pp., MIT Press, Cambridge, Mass., 1965.

Pelletier, J. D., Analysis and modeling of the natural variability of climate, *J. Clim., 10*, 1331-1342, 1997.

Peng, C.-K., S. V. Buldyrev, A. L. Goldberger, S. Havlin, F. Sciortino, M. Simons, and H. E. Stanley, Long-range correlations in nucleotide sequences, *Nature, 356,* 168-170, 1992.

Peng, C.-K., S. V. Buldyrev, S. Havlin, M. Simons, H. E. Stanley, and A. L. Goldberger, Mosaic organization of DNA nucleotides, *Phys. Rev. E, 49,* 1685-1689, 1994.

Press, W. H., S. A. Teukolsky, W. T. Vetterling, and B. P. Flannery *Numerical Recipes in Fortran,* 963 pp., Cambridge Univ. Press, New York, 1992.

Priestley, M. B., *Spectral Analysis and Time Series,* vol 1, 653 pp., Academic, San Diego, Calif., 1981.

Shea, D. J., The annual cycle, part I, The annual variation of surface temperature over the United States and Canada, *NCAR Tech. Note, NCAR/TN-242+STR,* 77 pp., Nat. Cent. for Atmos. Res., Boulder, Colo., 1984.

Stanley, H. E., L. A. N. Amaral, A. L. Goldberger, S. Havlin, P. Ch. Ivanov, and C.-P. Peng, Statistical Physics and physiology: Monofractal and multifractal approaches, *Physica A, 270,* 309-324, 1999.

Talkner, P., and R. O. Weber, Power spectrum and detrended fluctuation analysis: Application to daily temperatures, *Phys. Rev. E, 62,* 150-160, 2000.

Tsonis, A. A., P. J. Roebber, and J. B. Elsner, A characteristic time-scale in the global temperature record, *Geophys, Res. Lett., 25,* 2821-2823, 1998.

Vattay, G., and A. Harnos, Scaling behavior in daily air humidity fluctuations, *Phys. Rev. Lett., 73,* 768-771, 1994.

Weber, R. O., Influence of different daily mean formulas on monthly and annual averages of temperature, *Theor. Appl. Climatol., 47,* 205-213, 1993.

Weber R. O., P. Talkner, and G. Stefanicki, Asymmetric diurnal temperature change in the Alpine region, *Geophys. Res. Lett., 21,* 673-676, 1994.

P. Talkner and R. O. Weber, Paul Scherrer Institute, CH-5232 Villigen PSI, Switzerland. (peter.talkner@psi.ch)

(Received February 23, 2001; revised May, 17, 2001; accepted May 29, 2001.)